A numerical study on the critical bending moment for distortional buckling of cold-formed lipped C-sections

Vinícius Nogueira Magalhães[1], Adenilcia Fernanda Grobério Calenzani[1], João Victor Fragoso Dias[1]

[1]*Dept. of Civil Engineering, Federal University of Espírito Santo (UFES)*
Avenida Fernando Ferrari, 514, CEP 29075-910. Vitória / ES – Brazil.
vinicius.n.magalhaes@edu.ufes.br, adenilcia.calenzani@ufes.br, joao.v.dias@ufes.br

Abstract. Applications of cold-formed lipped C-sections have become more common in the civil construction industry. Frequently, these channels are submitted to bending about the major principal axis and, consequently, get under compression stresses that, due to the considerable sectional local slenderness, can provoke instability. Particularly complex, the distortional buckling is one of those failure modes and occur in these profiles causing translation of the edges. Thus, this article intends to numerically evaluate theoretical design procedures, when used to calculate the critical bending moment of distortional buckling. Four formulae were selected, and two computational approaches were employed to determine the critical moments in lipped C-sections: finite element method and finite strip method. Hancock's and Schafer's formulations proved to be highly precise when confronted with the numerical data. An adapted procedure presented by AISI showed itself imprecise, returning both unsafe and conservative results depending on the cross-section. The simplified method was conservative when predicting the distortional buckling moment. Conclusions regarding the critical moment and buckling modes with changes in geometrical parameters were also extracted. Thickness increase led the critical moment to grow. Likewise, as the lip width gets larger, the critical moment rises, however the profile tends to fail by local buckling mode.

Keywords: cold-formed lipped C-sections, distortional buckling, critical moment, finite element method, finite strip method.

1 Introduction

Cold-formed steel (CFS) is a promising trend on civil construction, that stand out for reducing on deadlines, simplifying assemblies and promoting lightweight buildings with high resistance capacity. El Kassas et al [1] confirm that, due to their lightweight, cold-formed sections are easier to transport in the field, minimizing costs related to lifting and execution. In Brazil, the use of CFS was stimulated in the decade of 1990, because of the scarcity of laminated profiles. Currently, their applications have become widely spread not only for roof purlins, but also when replacing conventional steel profiles with small dimensions, especially, in small scale buildings according to Choudrai [2].

The production of CFS, in line with the Brazilian National Standards Organization (ABNT) [3], consists of folding a sheet steel – produced by either hot or cold rolling – which allows the obtaining of varied sections, being simple or lipped C- and Z-sections the most common types. This process of folding is only viable on thin-walled shapes, that limits the thickness of the channels and promotes considerable local slenderness in CFS. Consequently, instability modes may occur in these structures, when they are under compression. Predominantly, these failure modes consist in the buckling of the profile walls comprising, in addition of displacements and rotations of the axis of the beam, distortion in the profile section. During manufacturing, lips can be added in the edge or in the

middle of the plates aiming to increase local resistance to these instability phenomena.

According to Dias et al [4], even though research on global buckling have started in 1700 and on local buckling in the early 1900s, only in the decade of 1970 progresses were achieved on distortional buckling due to computational advances. Distortional buckling (DB) is characterized as a rotation of the flange/lip assembly and, according to Schafer [5], it is more sensitive to dimensional imperfections than the local mode, evidencing the need of determining the efforts which cause this mode. ABNT [6] establishes the necessary requisites to be considered in the CFS design, in Brazil, and presents means for distortional buckling resistance calculation, through the Direct Resistance Method (DRM). In relation to obtaining the critical bending moment for DB, the code requires analysis based on the Theory of Elastic Stability.

Desmond [7], in 1977, created a theoretical design procedure by analyzing experimental data, which led him to incorporate distortional in local mode, considering the web slenderness, but also the stiffness of the web/flange assembly. Lau and Hancock [8], in 1987, continued to study the critical bending moment using the Finite Strip Method (FSM) and identified sections whose failure occurred by distortional buckling. Hancock [9] developed a procedure, based on a flange/lip thin-walled assembly under compression and on the stiffness of the profile web. Using the Finite Element Method (FEM), Schafer [5], in 1997, formulated a new model, analogous to Hancock's, but different when calculating an approximated stiffness of the interaction web/flange of cold-formed lipped C-sections. Schafer also concluded that channels which fail by distortion present less residual resistance than those that fail locally and proved that the American Iron and Steel Institute (AISI) [10] design procedure increases the critical moments. In 2010, AISI [11] devised a method derived from Schafer's: the Simplified Method. This method is applicable to sections with high web slenderness and flanges restricted by bracings or attachments, not considering the rotational stiffness of the flange. This procedure tends to be more conservative when used to calculate the distortional buckling stresses of unrestricted sections.

Because of the complex analytical solutions found in distortional buckling, studies require applications of an approximated numerical study generally solved by computer. Therefore, this article compiles different formulae, evaluating their limits, accuracies and implementation in usual design. Particularly, for this article, FEM and FSM are used to investigate cold-formed lipped C-sections under bending about the major principal axis.

2 Numerical models

For FEM and FSM calibration, an article was taken as a reference: Yu et al [12]. It was tried to achieve the same modeling procedure in FEM of Yu's research to confront the results obtained. Thus, the same properties were employed: modulus of elasticity $E = 205$ GPa, Poisson's ratio $\nu = 0{,}3$ and yield stress f_y = 390 MPa. The boundary conditions consisted in restricted translations in the directions y and z (see Fig. 1) and restricted rotation about the direction x (longitudinal axis) in one node of one end of the profile. The mesh was divided in elements sizes equal to 5 mm, which allows, simultaneously, accuracy and less computational costs. A concentrated bending moment were applied in the ends of the C-section bar. The model was made in ANSYS Mechanical APDL. The cross-section is exposed in Fig. 1 and the dimensions adopted by Yu et al [12] are listed in Tab. 2.

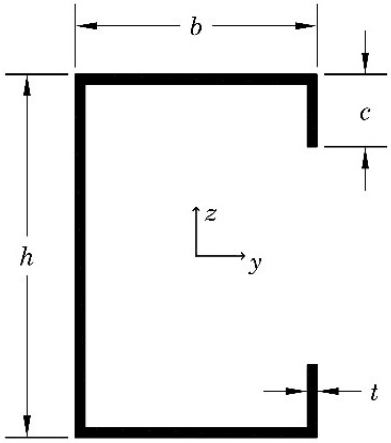

Figure 1. Profile section

SHELL181 elements were employed in the cross-section modeling. These elements have 4 nodes and 6 degrees of freedom per node, and they are based on Reissner-Mindlin shell theory. This approach enables the simulation of each profile plate which facilitate the determination of flexural modes to evaluating global, local and distortional modes. If the model was built with beam elements, local and distortional buckling could not be accounted for, because this element does not permit to visualize cross-sectional deformation. It was proceeded to a static analysis followed by an eigen buckling analysis, that returned ten eigen-values and ten eigen-vectors (related to the critical bending moment and the buckling modes). Figure 2 exemplifies a buckling mode obtained by FEM.

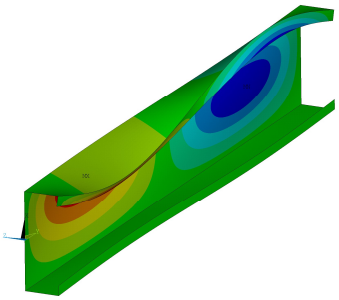

Figure 2. Example of distortional buckling mode of section 2

Concurrently, the FSM model was developed using CUFSM. The geometries applied were the same descripted in Fig. 1 and Tab. 2. Similarly to FEM, a concentrated bending moment was implemented in the profile ends. The span varied from 30 to 4000 mm, increasing 10 mm per iteration, permitting a better discretization of the characteristic curve of buckling. The critical bending moment was extracted from the pos-processor. In summary, Tab. 1 presents the critical bending moments determined by Yu et al [12] and by the developed FEM and FSM models, as well as the ratio between the results.

Table 1. Comparison between models

Section	Yu (kNcm)	FEM (kNcm)	FSM (kNcm)	Yu/FEM	Yu/FSM
1	1785.51	1671.10	1730.05	0.94	0.97
2	3545.06	3357.74	3451.94	0.95	0.97
3	6770.46	6365.89	6533.00	0.94	0.96

Small differences are observed between the reference and the numerical models. It occurs, due to divergences

in the modeling technique and to approximation errors by computer. However, the proposed models reflect high precise answers and are validated.

3 Results

Consecutive to the numerical model calibration, other eight sections were proposed to compose the phase of theoretical designs validation and parametric analysis. Their dimensions and critical bending moments are listed in the Tab. 2, below.

Table 2. Critical bending moments

Sec.	h (mm)	b (mm)	c (mm)	t (mm)	FEM (kNcm)	FSM (kNcm)	Hancock (kNcm)	Schafer (kNcm)	AISI (kNcm)	Simp. M. (kNcm)
1	150	50	15	2	1671.1	1730.0	1646.7	1619.6	2348.3	279.7
2	200	70	20	2.5	3357.7	3451.9	3299.7	3233.3	3770.3	597.4
3	250	80	25	3	6365.9	6533.0	6203.7	6086.3	8292.8	1095.5
4	200	100	33.33	2	2593.2	2593.2	2297.7	2413.0	1665.6	904.5
5	200	100	33.33	3	5889.8	6020.8	5429.0	5631.3	5347.5	1730.5
6	200	100	25	2	1938.3	1983.9	1902.3	1901.5	1700.1	558.5
7	200	100	25	3	4555.3	4663.3	4529.6	4504.4	4518.4	1125.9
8	200	66.67	22.22	2	2339.5	2400.5	2239.2	2219.0	2675.0	490.7
9	200	66.67	22.22	3	5576.6	5726.9	5352.1	5360.9	9490.8	938.8
10	200	66.67	16.67	2	1848.2	1897.5	1847.2	1775.0	2251.0	318.0
11	200	66.67	16.67	3	4498.9	4624.3	4491.7	4044.7	7269.0	608.7

Table 3 informs the ratio between the theoretical and numerical results obtained by FEM and FSM, as well as the average, standard deviation (s) and coefficient of variation (CV) for each formula.

Table 3. Comparison between numerical and theoretical results

Sec.	Hancock		Schafer		AISI		Simplified M.	
	FEM	FSM	FEM	FSM	FEM	FSM	FEM	FSM
1	0.99	0.95	0.97	0.94	1.41	1.36	0.17	0.16
2	0.98	0.96	0.96	0.94	1.12	1.09	0.18	0.17
3	0.97	0.95	0.96	0.93	1.20	1.27	0.17	0.17
4	0.89	0.89	0.93	0.93	0.64	0.64	0.35	0.35
5	0.92	0.90	0.96	0.94	0.91	0.89	0.29	0.29
6	0.98	0.96	0.98	0.96	0.88	0.86	0.30	0.30
7	0.99	0.97	0.99	0.97	0.99	0.97	0.25	0.24
8	0.96	0.93	0.95	0.92	1.14	1.11	0.21	0.20
9	0.96	0.93	0.96	0.94	1.70	1.66	0.17	0.16
10	1.00	0.97	0.96	0.94	1.22	1.19	0.17	0.17
11	1.00	0.97	0.98	0.95	1.62	1.57	0.14	0.13
Average	0.9674	0.9443	0.9731	0.9403	1.1754	1.1459	0.2178	0.2131
s	0.0352	0.0286	0.0163	0.0129	0.3200	0.3071	0.0699	0.0702
CV	3.64%	3.03%	1.69%	1.37%	27.23%	26.80%	32.07%	32.93%

Hancock's and Schafer's procedures converged to high precision answers compared to the numerical model results, presenting averages of 94%, at least, and coefficients of variation lower than 4%. These theoretical models are more realistic than the others, because they consider the stiffness of the web/flange interaction. AISI increased the critical bending moment of sections 1, 3, 9, 10 and 11, in line with Schafer [5], and led to good approximations in sections 2, 6 and 7, reasonable estimates were found for 5 and 8. Although, this formulation decreased the moment for section 4. It reflected in an average of 115% and in a considerable coefficient of variation close to 27%. The unpredictability of AISI's equation occurs, due to its conception, based on local buckling and, subsequently, adapted for distortional buckling. In parallel, for all sections, the Simplified Method diverged,

conducting to decreased moments, as predicted in AISI [11]. This reduction happens, because this procedure gets conservative when supposing bracings on the superior flange – boundary condition no specified in the numerical model. The average was 21% of the numerical results and the coefficient of variation equal to 32%. Figure 3 resumes the theoretical and numerical results.

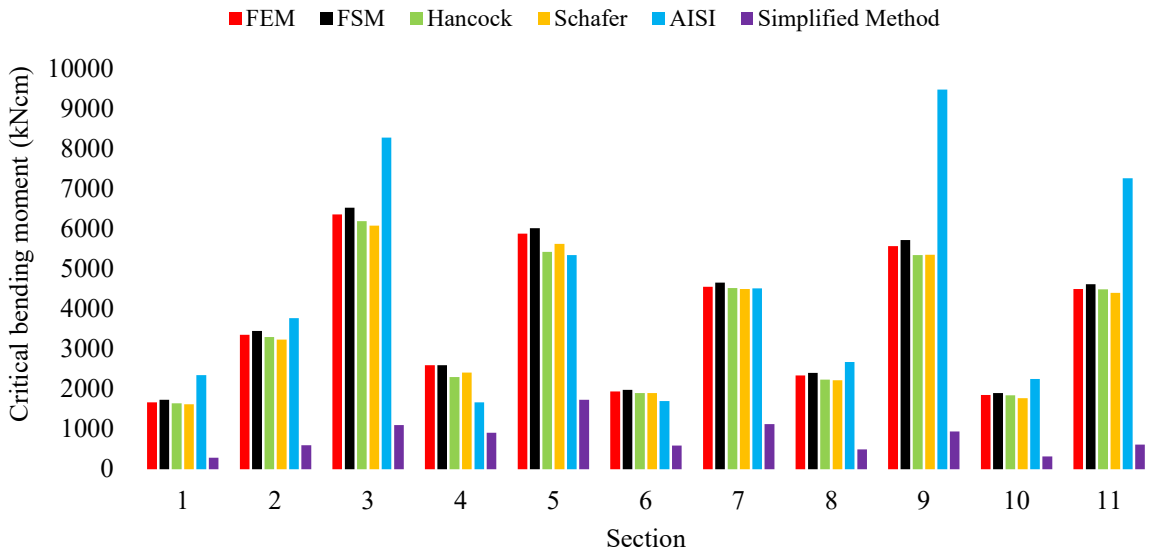

Figure 3. Numerical and theoretical critical bending moments

Then, a parametric analysis was made: the geometric properties were fixed, except one, aiming to identify a pattern in the critical bending moment behavior. The results are illustrated in Figs. 4 and 5, representing the bending moment non-dimensionally, dividing the critical moment by the first yield moment, considering $f_y = 390$ MPa.

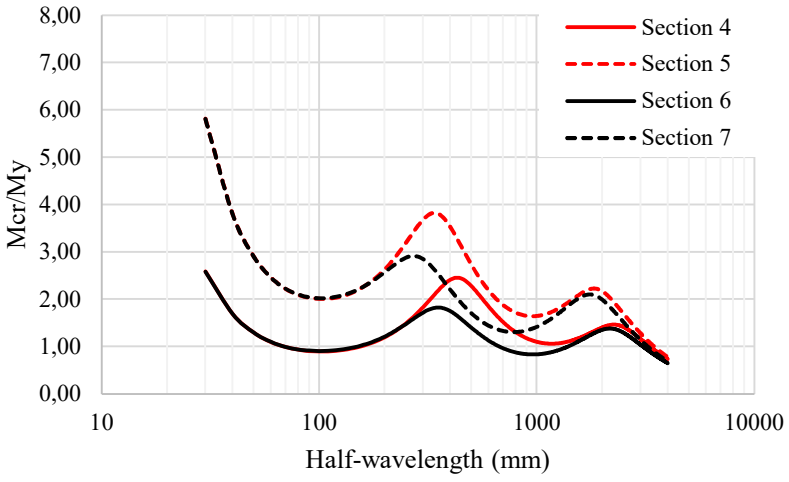

Figure 4. Behavior of the critical bending moment for parameters manipulation (sec. 4-7)

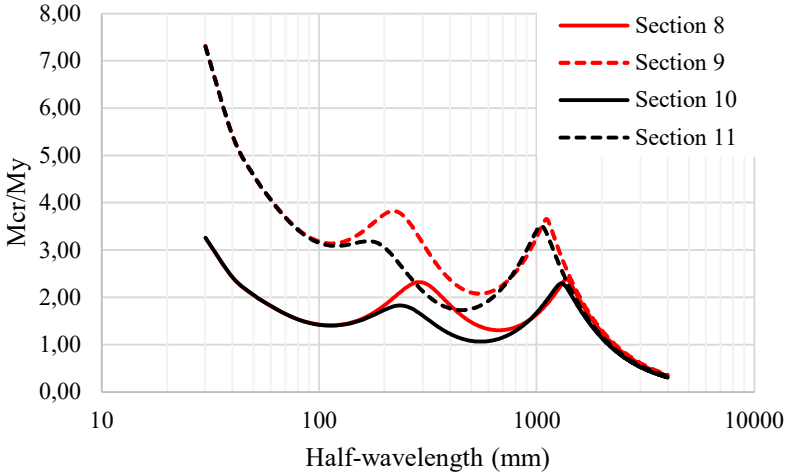

Figure 5. Behavior of the critical bending moment for parameters manipulation (sec. 8-11)

Through the Fig. 4 and 5, it was noted that adding 1 mm in thickness, the critical stress rose over 50% of the initial stress. It occurs, because an increment in thickness reduces the local slenderness of the profile walls – web/thickness (h/t) and flange/thickness (b/t) –, gaining stiffness in the web/flange assembly, which governs DB. Continuously, as the thickness grows, stiffness is gained and, consequently, the critical moment for DB gets bigger. Conclusions about the lip length were made. It was observed that when it was reduced by 25%, the stress decreased. It was expected, since the critical moment rises as the lip length gets close to the flange width. Thus, as the lip/flange ratio converges to 1, there is an increment of DB resistance, due to a gain of stiffness in the cross-section, according to AISI [10]. Particularly, in this case, the lip/flange ratio changed from 0.33 to 0.25, reducing the critical bending moment. It should be noted though that an excessively wide lip may result in local buckling of the lip becoming critical.

Table 4 presents the sensibility of the critical stress when manipulating these parameters. Regarding to thickness, the critical stress increased in percentage of 51 to 62%. In terms of the reduction in the lip length, the stress decreased in percentage of 17 to 23%.

Table 4. Critical normal stress variation due to parameters variation

Thickness manipulation		Lip length manipulation	
Ratio	Effect on the stress	Ratio	Effect on the stress
$\sigma_{cr,5}/\sigma_{cr,4}$	1,51	$\sigma_{cr,6}/\sigma_{cr,4}$	0,77
$\sigma_{cr,7}/\sigma_{cr,6}$	1,57	$\sigma_{cr,7}/\sigma_{cr,5}$	0,79
$\sigma_{cr,9}/\sigma_{cr,8}$	1,59	$\sigma_{cr,10}/\sigma_{cr,8}$	0,81
$\sigma_{cr,11}/\sigma_{cr,10}$	1,62	$\sigma_{cr,11}/\sigma_{cr,9}$	0,83

4 Conclusions

In this article, theoretical designs procedures of distortional buckling determination were evaluated. Numerical analysis by FEM and FSM were employed and taken as reference for this research, confronting theoretical and numerical results.

For equations studies, spreadsheets in Microsoft Excel were developed to determinate the critical bending moment. Hancock's and Schafer's designs presented high precisions when compared to the numerical models, given that are methods that comprise more parameters in the procedure, in other words, they analyze DB instability based a flange/lip assembly adding a web/flange stiffness. Generally, Schafer showed itself a better formulation than Hancock. AISI was configured as unpredictable, assuming thar for six section the answer diverged and for

the others, it was acceptable. Despite the average is just 15% greater than the numerical results, the coefficient of variation is big, leading to bad accuracies. The Simplified Method, which ignore the web/flange stiffness, decreased the moment confirming itself as a conservative procedure. Its coefficient of variation was high. Therefore, it is recommended the use of Hancock's and Schafer's equation, due to their stringency.

Furthermore, geometric parameters affect the critical bending moment for DB. It was observed that sections with thickness equals to 3 mm are more resistant than those with 2 mm, because this addition reduces the web slenderness, increasing the stiffness and, consequently, the moment. By evaluating the lip length, it was noted an increment in the resistance, when the length is amplified, due a gain in the cross-section stiffness.

Acknowledgements. The authors acknowledge the Federal University of Espírito Santo, the Brazilian Federal Government Agency CAPES and State Government Agency FAPES for the financial support provided during the development of this study. The second author thanks the State Government Agency FAPES for the research productivity grant.

Authorship statement. The authors hereby confirm that they are the sole liable persons responsible for the authorship of this work, and that all material that has been herein included as part of the present paper is either the property (and authorship) of the authors, or has the permission of the owners to be included here.

References

[1] E. M. A. El-Kassas, I. R. Mackie and A. I. El-Sheikh, "Using neural networks in cold-formed steel design". *Computers and Structures*, vol. 79, 2001.
[2] G. M. de B. Choudrai. Análise teórica e experimental de perfis de aço formados a frio submetidos à compressão. PhD thesis, São Paulo University, 2006.
[3] ABNT, "NBR 6355, Perfis estruturais de aço formados a frio: Padronização", ABNT, 2012.
[4] J. V. F. Dias, A. F. G. Calenzani and R. H. Fakury, "Elastic Critical Moment of Lateral-Distortional Buckling of Steel-Concrete Composite Beams under Uniform Hogging Moment". *International Journal of Structural Stability and Dynamics*, vol. 19, n. 7, 2019.
[5] B. W. Schafer. Cold-Formed Steel Behavior and Design: Analytical and Numerical Modeling of Elements and Members with Longitudinal Stiffeners. PhD thesis, Cornell University, 1997.
[6] ABNT, "NBR 14762: Dimensionamento de estruturas de aço constituídas por perfis formados a frio", ABNT, 2010.
[7] T. P. Desmond. The Behavior and Strength of Thin-Walled Compression Elements with Longitudinal Stiffeners. PhD thesis, Cornell University, 1977.
[8] S. C. W Lau and G. J. Hancock, "Distortional Buckling Formulas for Channel Columns". *Journal of Structural Engineering*, vol. 113, n. 5, pp. 1063-1078, 1987.
[9] G. J. Hancock, "Design for Distortional Buckling for Flexural Members". Thin-Walled Structures, vol. 27, n. 1, pp. 3-12, 1997.
[10] AISI, "Distortional Buckling of Cold-Formed Steel Columns", AISI, 2020.
[11] AISI, "S100-16: North American Specification for the Design of Cold-Formed Steel Structural Members", AISI, 2016.
[12] N. -t. Yu, B. Kim, W. -b. Yuan, L. -y. Li and F. Yu, "An analytical solution of distortional buckling resistance of cold-formed steel channel-section beams with web openings". *Thin-Walled Structures*, vol. 135, pp. 446-452, 2019.